Journal of Vacuum Science and Technology B

RESEARCH ARTICLE | FEBRUARY 13 2024

High sensitivity saliva-based biosensor in detection of breast cancer biomarkers: HER2 and CA15-3

Hsiao-Hsuan Wan ; Haochen Zhu ; Chao-Ching Chiang ; Jian-Sian Li ; Fan Ren ; Cheng-Tse Tsai; Yu-Te Liao; Dan Neal ; Josephine F. Esquivel-Upshaw ; Stephen J. Pearton

J. Vac. Sci. Technol. B 42, 023202 (2024)
https://doi.org/10.1116/6.0003370

JVST B
Journal of Vacuum Science & Technology B

ARTICLE

pubs.aip.org/avs/jvb

High sensitivity saliva-based biosensor in detection of breast cancer biomarkers: HER2 and CA15-3

Cite as: J. Vac. Sci. Technol. B **42**, 023202 (2024); doi: 10.1116/6.0003370
Submitted: 7 December 2023 · Accepted: 3 January 2024 ·
Published Online: 13 February 2024

Hsiao-Hsuan Wan,[1,a)] Haochen Zhu,[1] Chao-Ching Chiang,[1] Jian-Sian Li,[1] Fan Ren,[1] Cheng-Tse Tsai,[2] Yu-Te Liao,[2] Dan Neal,[3] Josephine F. Esquivel-Upshaw,[4] and Stephen J. Pearton[5]

AFFILIATIONS

[1]Department of Chemical Engineering, University of Florida, Gainesville, Florida 32611
[2]Department of Electronics and Electrical Engineering, National Yang Ming Chiao Tung University, Hsinchu 30010, Hsinchu, Taiwan
[3]Department of Surgery, University of Florida, Gainesville, Florida 32610
[4]Department of Restorative Dental Science, Division of Prosthodontics, University of Florida, Gainesville, Florida 32611
[5]Department of Materials Science and Engineering, University of Florida, Gainesville, Florida 32611

[a)]**Electronic mail:** hwan@ufl.edu

ABSTRACT

The prevalence of breast cancer in women underscores the urgent need for innovative and efficient detection methods. This study addresses this imperative by harnessing salivary biomarkers, offering a noninvasive and accessible means of identifying breast cancer. In this study, commercially available disposable based strips similar to the commonly used glucose detection strips were utilized and functionalized to detect breast cancer with biomarkers of HER2 and CA15-3. The results demonstrated limits of detection for these two biomarkers reached as low as 1 fg/ml much lower than those of conventional enzyme-linked immunosorbent assay in the range of 1~4 ng/ml. By employing a synchronized double-pulse method to apply 10 of 1.2 ms voltage pulses to the electrode of sensing strip and drain electrode of the transistor for amplifying the detected signal, and the detected signal was the average of 10 digital output readings corresponding to those 10 voltage pulses. The sensor sensitivities were achieved approximately 70/dec and 30/dec for HER2 and CA15-3, respectively. Moreover, the efficiency of this novel technique is underscored by its swift testing time of less than 15 ms and its minimal sample requirement of only 3 μl of saliva. The simplicity of operation and the potential for widespread public use in the future position this approach as a transformative tool in the early detection of breast cancer. This research not only provides a crucial advancement in diagnostic methodologies but also holds the promise of revolutionizing public health practices.

I. INTRODUCTION

Breast cancer, the most frequently detected cancer globally, had over 2.3 million new cases and resulted in approximately 685 000 deaths in the year 2020. In the U.S. alone, in 2022, approximately 287 850 new cases of invasive breast cancer and 51 400 cases of ductal carcinoma *in situ* (DCIS) were diagnosed among women, leading to 43 250 female deaths from breast cancer.[1] The future impact of breast cancer is expected to escalate, with projected figures estimating over 3 million new cases and approximately 1 million deaths in the year 2040.[2,3] Imaging techniques such as mammography, ultrasound, and/or magnetic resonance imaging (MRI), and biopsies are the gold standard procedures for breast cancer diagnosis.[4,5] However, these methods have many disadvantages such as high cost, limited accessibility, inaccuracies in detecting early-stage cancer in young women with denser breast tissue, invasiveness, low-dose radiation exposure, especially for patients who are sensitive to radiation. In addition, there is a need for specialized equipment and additional support from technologists and radiologists. ELISA-based testing of HER2 and/or CA15-3 in serum are essential biomarkers used in breast cancer diagnosis, treatment selection, and monitoring response to targeted therapies used to screen or monitor breast cancer in conjunction with those invasive methods mentioned above.[6] HER2 (ERBB2, HER-2/neu) is a protein that plays a significant role in normal cell growth and

division. However, in approximately 15%–20% of breast cancer cases, there is an overexpression or amplification of the HER2 gene, leading to an increased amount of HER2 protein on the surface of cancer cells. This overexpression is associated with aggressive tumor growth, higher recurrence rates, and poorer prognosis. CA15-3 is a tumor-associated antigen that can be detected in the blood of some breast cancer patients. Elevated levels of CA15-3 may indicate the presence of cancer cells and can be used as a complementary tool alongside other diagnostic tests and imaging techniques.[7–11] The concentrations of HER2 and CA15-3 in saliva can be correlated to their concentrations in serum, thus saliva samples can also be employed for breast cancer detection.[7,8,10] The binding constants for these two biomarkers, HER2 and CA15-3, are 0.32 μM and 0.135 nM, respectively.[12,13] However, the ELISA-based detections of HER2 and CA15-3 require trained technicians and one to two weeks to obtain results. Furthermore, the limit of detection of ELISA is only around 10^{-8}~10^{-10} g/ml.[14,15] A more efficient and cost-effective alternative is the utilization of biosensors for the detection of breast cancer tumor markers.[9]

In recent years, field-effect transistor (FET)-based biosensors have received much attention for biomolecular detection due to their high sensitivity, label-free detection, and rapid real-time options. In addition, detection devices based on FETs could show both qualitative and quantitative results in a short time.[16–18] There are several kinds of FETs, such as silicon nanowire FET (SiNW-FET), graphene FET (gFET), Si metal-oxide-semiconductor field-effect transistors (MOSFETs), and tunneling FET (TFET) that have been used as part of biosensor devices to amplify the detected signals.[19–26]

Instead of using the transistors as the sensors, which need to be disposed of after each use, a system with a reusable printed circuit board (PCB) containing a MOSFET and disposable test strips were employed. In this approach, synchronized double-pulses were applied at the gate and drain terminals of the transistor to ensure that the channel charge does not accumulate, and there is no need to reset the drain and gate paths to mitigate the charge accumulation at the gate and drain of the sensing transistor for sequential testing. With the double-pulse approach, it only takes a few seconds to show the result of the test, due to the rapid response of the functionalized test strips and resulting electrical signal output. As an example, the LoD has been demonstrated to reach 10^{-15} g/ml and the sensitivity to 78/dec for COVID-19 detection. Similar approaches have been used to detect cerebrospinal fluid (CSF), cardiac troponin I, and Zika virus.[27–30]

In this work, use of this double-pulse measurement approach to detect HER2 and CA15-3 in saliva samples collected from healthy volunteers and breast cancer patients was investigated. The voltage output responses of the transistor correlated to the HER2 and CA15-3 concentrations, detection limits, and sensing sensitivity were determined.

II. EXPERIMENT

The test strips used in this research are the ones commercially available for glucose tests as shown in Fig 1(a). The strips were made by Luvnshare Biomedical Inc. in Hsinchu, Taiwan. The method of functionalizing the strips was described in detail in a previous publication.[31,32] Briefly, the first step is to plate the carbon electrodes with gold by connecting to the gate pulse source on the PCB board. The strips are then immersed into 10 mM thioglycolic acid (TGA) solution for 4h to form strong Au–S bonds on the gold plated electrode. After this, the strips are soaked in N, N′-dicyclohexylcarbodi-imide (0.1 mM) and N-hydroxysuccinimide (0.1 mM) in acetonitrile for 2 h. 20 μg/ml anti-HER2/ ERBB2 monoclonal antibody (Sino Biological Inc., Chesterbrook, PA) is then injected into the microchannel after which the strips are stored in a sealed disk for 18 h under 4 °C. For the test of CA15-3 (MUC1), the same steps are followed for the HER2 process, with the exception of using CA15-3 monoclonal antibody (Sino Biological Inc., Chesterbrook, PA) for the last step. Finally, ethanolamine is used to terminate the unfunctionalized groups to prevent interference. To relate our results into real concentration numbers, the HER2 and CA15-3 proteins were diluted serially in saliva and stored at 4 °C before use. All the

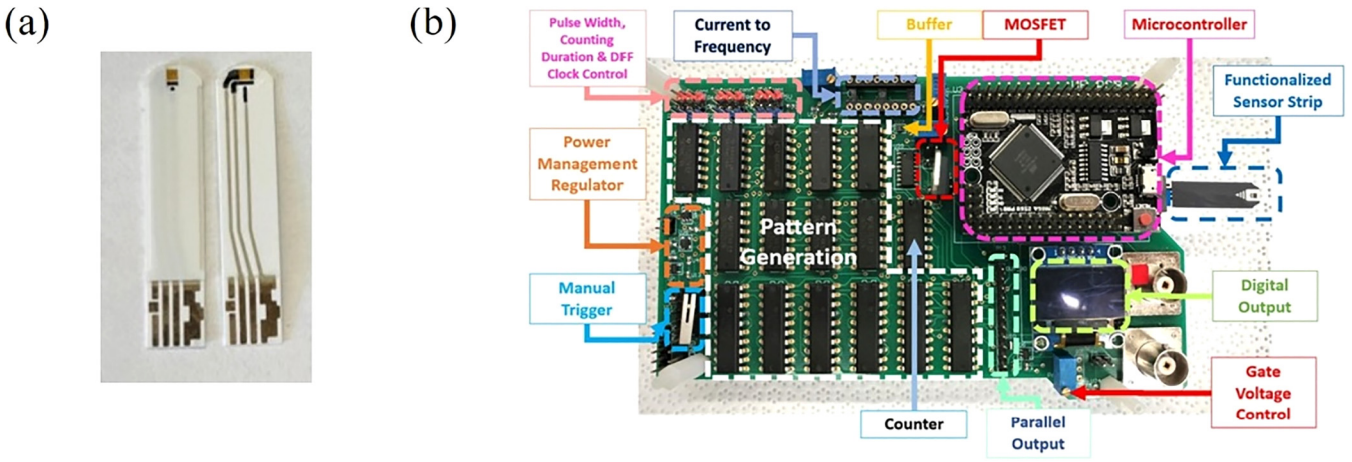

FIG. 1. (a) Schematic of the test strips with cover (left) and without cover (right). (b) Printed circuit board to generate digital reading.

antibodies employed in this study went through the validation process to show their specificity of binding to the specific protein.[33,34] We also used the sensor strips functionalized with HER2 antibody to sense different CA15-3 and conversely utilizing strips functionalized with CA15-3 antibody to detect HER2. There was no response for either of those cases, and the output readings were similar to the ones for blank saliva.

A printed circuit board (PCB) as illustrated in Fig. 1(b) was designed to convert the detected voltage signals related to the strips into digital readings. A MOSFET (STMicroelectronics STP200N3LL) was used to amplify the detected signal from the test strip. Synchronous voltage pulses are sent to both the electrode of the strip connecting to the gate and drain electrodes of the MOSFET. The drain pulse is applied for around 1.1 ms at a constant voltage. The gate pulse starts at 40 μs after the drain pulse and ends at 40 μs before the end of the drain pulse. A variable resistor is connected to the drain as the load resistor.

In addition to obtaining the calibration curve from a series of diluted proteins, 17 human saliva samples from both breast cancer patients and 4 control samples from healthy volunteers were obtained through the University of Florida Clinical and Translational Science Institute (UF CTSI) Biorepository. These samples were collected from patients within the University of Florida Health System and were preserved in a −78 °C freezer. These deidentified samples all came with corresponding diagnoses, which were confirmed through biopsies as part of the patients' routine care (UF IRB202101643). After defrosting, the saliva samples were applied to the microfluidic channel directly without dilution, filtration, or centrifugation. Based on the histologic type, the human samples were classified into three groups: (1) healthy control, (2) in situ breast cancer, and (3) invasive breast cancer. Among the invasive breast cancer samples, one of them was HER2-positive, while the rest of the samples were HER2-negative tested through biopsy results using immunohistochemistry (IHC). All the samples were tested with two different types of strips, which were functionalized with either HER2 or CA15-3. All of the output digital readings were averaged from 10 pulse measurements, which took around 15 ms. The p-values of test results were analyzed with both the Kruskal–Wallis test.

III. RESULTS AND DISCUSSION

To verify the authenticity of the sensor and its ability to detect HER2 protein, the biofunctionalized strips initially underwent testing using pure HER2 protein (Sino Biological Inc., Chesterbrook, PA) that was successively diluted to different concentrations. The dilutions ranged from pure artificial saliva (Pickering Laboratories Inc., Mountain View, CA), to a minimum dilution of 1×10^{-15} g/ml in artificial saliva. Figure 2(a) depicts dynamic drain output voltage waveforms at various concentrations ranging from 1 fg/ml to 10 μg/ml during each gate pulse. To convert the analog voltage signals to digital signals, the drain voltage levels at fixed 750 μs were extracted from each curve and transformed into digital signals through a voltage-controlled oscillator (VCO) on the PCB board. As shown in Fig. 2(b), a sensitivity of 70/dec was achieved with a limit of detection (LOD) of 10^{-15} g/ml,[30–32,35–37] which was four orders lower than the gold standard ELISA test, which is around 10^{-8}–10^{-10} g/ml,[15,38] used to measure these biomarkers. The sensitivity is defined as the drop in digital reading when the protein concentration increases by one order. Logarithmic scales are useful because they compress a wide range of values into a more manageable scale. To ensure the repeatability and reliability of the measured results, the curve was refined by averaging 10 consecutive identical pulse measurements. The total measurement time of 10 pulses is under 15 ms, hence, this technique holds promise for real-time point-of-service applications.

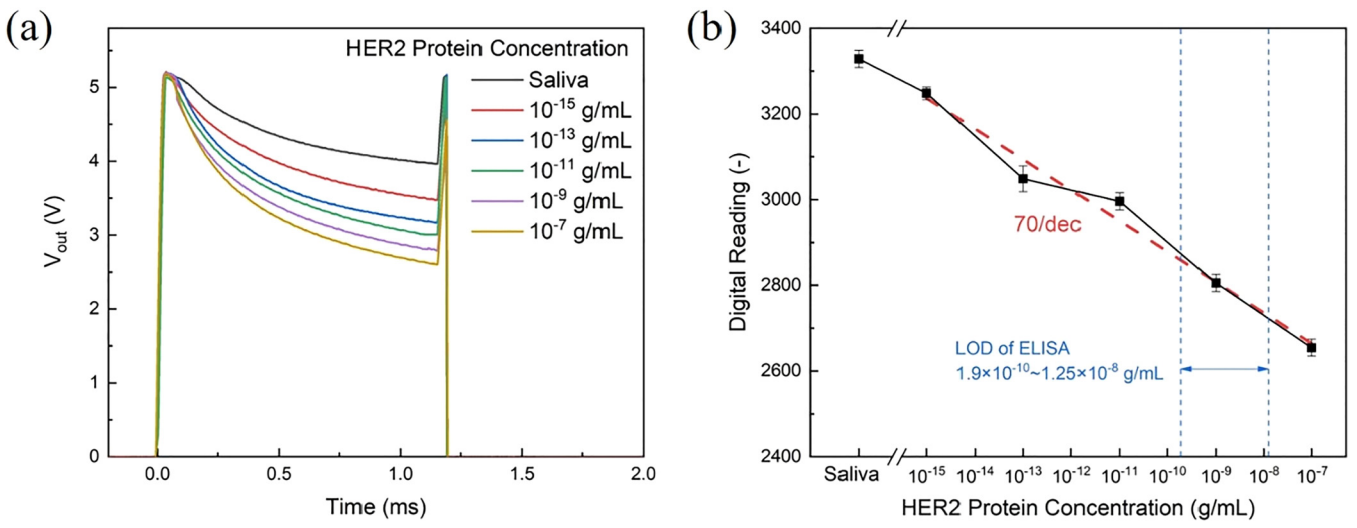

FIG. 2. (a) Output drain voltage waveform for pure artificial saliva and HER2 protein diluted in saliva from 10^{-7} to 10^{-15} g/ml. (b) Output digital reading from PCB under different HER2 protein concentrations. The limit of detection is 10^{-15} g/ml while the sensitivity is 70/dec. The LOD of ELISA data is taken from Ref. 15.

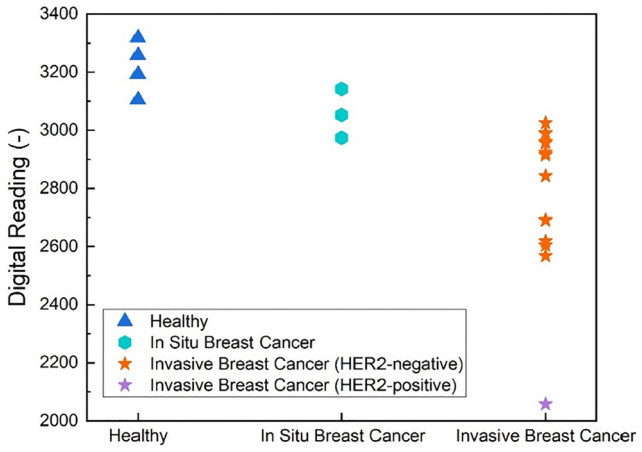

FIG. 3. Output digital reading result from the human sample test with strips functionalized by HER2 antibody. The orange star stands for HER2-negative cases, which are all the stars except for the lowest reading one. The purple star indicates the HER2-positive case, it shows the lowest reading as the HER2 concentration is way higher than other cases.

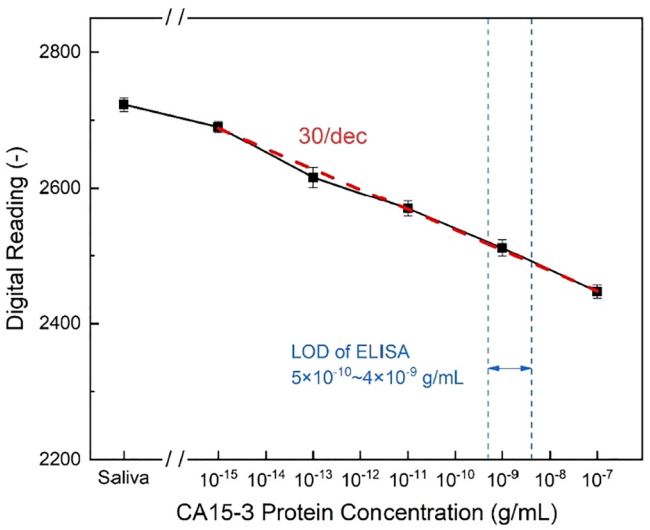

FIG. 4. Average output digital reading from PCB with different CA15-3 protein concentrations. The limit of detection is 10^{-15} g/ml while the sensitivity is 30/dec. The LOD of ELISA data is taken from Ref. 14.

Previously described and modeled, the antigen-antibody complexes undergo stretching and contracting, akin to double springs, in response to a pulsed gate electric field.[30] This motion across the antibody-antigen structure, corresponding to the pulse voltage applied on the test strip, induces an alteration in the protein's conformation, resulting in a time-dependent electric field applied to the MOSFET gate. Consequently, a springlike pattern emerges in the drain voltage waveform due to the external connection between the sensor strip and the MOSFET's gate electrode. In Fig. 2(b), an observable trend emerges where increased spike antigen concentration of HER2, induces a consistent reduction in drain output voltage and a subsequent decrease in the digital reading.[31,32,39]

Figure 3 shows output digital readings of 21 human saliva samples, where there are clear differences among healthy, *in situ* and invasive breast cancer cases. *In situ* ductal carcinoma breast cancer is a type of cancer confined in a milk duct, which eventually grows into the rest of the breast tissue. Invasive breast cancer, is a type of cancer, which has spread into the surrounding breast tissue. Table I shows the median and the range of digital readings by disease status and overall *p*-value using the Kruskal–Wallis test to examine if there exist statistically significant distinctions among two or more groups. The overall *p*-value is significant while the value for HER2 is 0.002, which show the probability of false-positive detection. This indicates that this sensor technology is an efficient way to detect HER2 biomarkers in saliva. Immunohistochemistry (IHC), which was the test used to determine HER2 status on our patients, is a special staining process performed on fresh or frozen breast cancer tissue removed during biopsy to show whether or not the cancer cells have too much HER2 receptors and/or hormone receptors on their surface.[40,41] IHC is a qualitative test based loosely off of eye scored counting and gives a score of 0 to 3+ for the amount of HER2 receptor protein on the surface of cells in a breast cancer tissue sample. For example, 0 to 1+ is HER2-negative, 2+ is the borderline and is confirmed positive using fluorescence *in situ* hybridization (FISH) and, 3+ is HER2-positive. Among 17 saliva samples, there is only one HER2-positive sample and the rest of the 16 samples were HER2-negative, 0 or +1. For HER2-positive cases, cancers tend to grow and spread faster than breast cancers that are HER2-negative, but are much more likely to respond to treatment with drugs that target the HER2 protein. By using sensor technology presented in this work, no invasive biopsy is required to determine the HER2 concentration. ELISA can only be used to confirm the cancer status of the HER2-positive sample but not the HER2-negative samples because this test is not sensitive enough to detect the HER2 antibody for the majority of HER2-negative samples. These data clearly show that this sensor technology has the potential to be used to identify the presence of breast cancer regardless of whether the samples are HER2-negative or -positive.

TABLE I. Median (range) by disease status. *p*-Values are the results of Kruskal–Wallis tests (overall).

	Healthy volunteers ($N = 4$, 19%)	*In situ* breast cancer ($N = 3$, 14%)	Invasive breast cancer ($N = 14$, 67%)	*p*-value
HER2	3226 (3105, 3318)	3053 (2974, 3142)	2879 (2058, 3025)	0.002
CA15-3	2620 (2589, 2673)	2496 (2378, 2623)	2356 (2108, 2575)	0.005

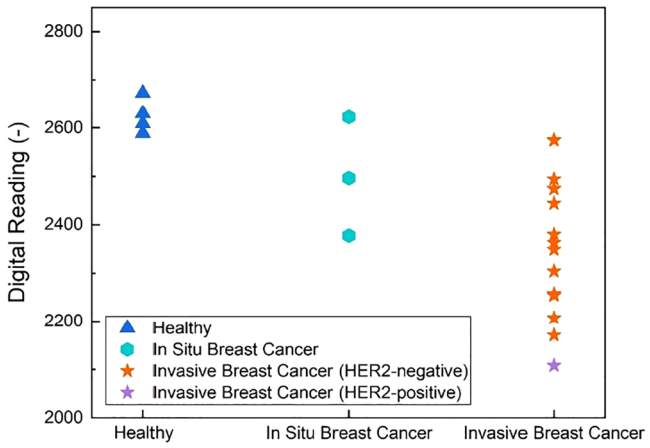

FIG. 5. Output digital reading result from the human sample test with strips functionalized by CA15-3 antibody.

Another cancer antigen, CA15-3, is used as a surrogate marker to monitor metastatic breast cancer patients undergoing treatment and for the preclinical detection of tumor recurrence. Levels of CA 15-3 have a significant relationship to outcome in patients with early breast cancer and are commonly used to detect breast cancer or monitor the effectiveness of cancer treatments. Detection of both CA15-3 and HER2 at the same time to ascertain breast cancer progression was strongly suggested.[42,43] Figure 4 illustrates the calibration curve for the CA15-3 biomarker and a LOD of 10^{-15} g/ml with a sensitivity of 30/dec was demonstrated. The sensitivity of detecting CA15-3 is less than half of the sensitivity for HER2, which is 70/dec. This is due to the molecular weight of CA15-3 protein, 250~350 kDa, which is much larger than that of the HER2 protein, 185 kDa.[44,45] According to the double spring model proposed in our previous work, in order to simulate the output voltage responses, the disparity in size between the HER2 molecule and CA15-3 would produce a larger spring constant for CA15-3 molecule and diminish the detection sensitivity of CA15-3.

In Fig. 5, the test results for detecting CA15-3 of the human samples are displayed. The digital reading decreases from the healthy group to the invasive breast cancer group, indicating an increase in CA15-3 concentration. The median, the range by disease status, and overall *p*-values analyzed with the Kruskal–Wallis test for the CA15-3 test are listed in Table I. The overall *p*-value for CA15-3 is 0.005, indicating that this device provides an efficient way to detect the salivary biomarkers related to breast cancer.

IV. SUMMARY AND CONCLUSIONS

This study demonstrated an effective approach for identifying salivary biomarkers linked to breast cancer. The method employed a hand-held size PCB to provide synchronized voltage pulses applied to a commercially available test strip, similar to the glucose detecting strip and the drain electrode of the transistor on PCB, while the transistor on the board was used to amplify the detected signal. This saliva-based noninvasive test, which leveraged biomarkers like HER2 and CA15-3, revealed impressive limits of detection (LOD) and sensitivity. Both HER2 and CA15-3 biomarkers exhibited an exceptional LOD as low as 1 fg/ml, surpassing ELISA kits by four orders of magnitude. This improved LOD facilitates the distinction of HER2-negative cases. HER2 sensitivity was determined to be 70/dec, and CA15-3 sensitivity was 30/dec with diluted proteins. These established relationships allow us to correlate test results into relative protein concentrations. Moreover, the noninvasive test was performed 10 times within 15 ms and the whole test took less than a minute to perform, including applying 3–5 μl saliva sample on the strip. The method is user-friendly and holds significant promise for widespread use by the general public in the future.

ACKNOWLEDGMENTS

This research was partially funded by NIH-NIDCR Grant (No. R56 DE025001). The authors at National Yang Ming Chiao Tung University, Hsinchu 30010, Taiwan would like to acknowledge the National Science and Technology Council, Taiwan, for their financial support under Grant No. NSTC 112-2628-E-A49-015.

AUTHOR DECLARATIONS

Conflict of Interest

The authors have no conflicts to disclose.

Ethics approval

Ethics approval for experiments reported in the submitted manuscript on animal or human subjects was granted. Human samples were obtained through the University of Florida Clinical and Translational Science Institute (UF CTSI) Biorepository. These deidentified samples all came with corresponding diagnoses, which were confirmed through biopsies as part of the patients' routine care (UF IRB202101643).

Author Contributions

Hsiao-Hsuan Wan: Data curation (equal); Formal analysis (equal); Investigation (equal); Methodology (equal); Validation (equal); Visualization (equal); Writing – original draft (equal). **Haochen Zhu:** Data curation (equal); Formal analysis (equal); Investigation (equal); Methodology (equal); Validation (equal); Visualization (equal). **Chao-Ching Chiang:** Investigation (equal); Methodology (equal); Validation (equal). **Jian-Sian Li:** Methodology (equal); Validation (equal). **Fan Ren:** Conceptualization (equal); Funding acquisition (equal); Project administration (equal); Resources (equal); Supervision (equal); Writing – review & editing (equal). **Cheng-Tse Tsai:** Methodology (equal); Software (equal); Validation (equal). **Yu-Te Liao:** Conceptualization (equal); Funding acquisition (equal); Project administration (equal); Resources (equal); Writing – review & editing (equal). **Dan Neal:** Methodology (equal); Software (equal). **Josephine F. Esquivel-Upshaw:** Conceptualization (equal); Funding acquisition (equal); Methodology (equal); Project administration (equal); Resources (equal); Supervision (equal); Writing – review & editing (equal). **Stephen J. Pearton:** Conceptualization (equal); Funding acquisition (equal); Project administration (equal); Writing – review & editing (equal).

DATA AVAILABILITY

The data that support the findings of this study are available within the article.

REFERENCES

[1]A. N. Giaquinto, H. Sung, K. D. Miller, J. L. Kramer, L. A. Newman, A. Minihan, A. Jemal, and R. L. Siegel, Cancer J. Clin. **72**, 524 (2022).
[2]M. Arnold *et al.*, The Breast **66**, 15 (2022).
[3]The American Cancer Society medical and editorial content team, *Key Statistics for Breast Cancer* (2023) see https://www.cancer.org/cancer/types/breast-cancer/about/how-common-is-breast-cancer.html.
[4]S. H. Jafari, Z. Saadatpour, A. Salmaninejad, F. Momeni, M. Mokhtari, J. S. Nahand, M. Rahmati, H. Mirzaei, and M. Kianmehr, J. Cell. Physiol. **233**, 5200 (2018).
[5]L. E. Pace and N. L. Keating, JAMA **311**, 1327 (2014).
[6]N. Samy, H. M. Ragab, N. A. El Maksoud, and M. Shaalan, Cancer Biomark. **6**, 63 (2010).
[7]F. Laidi, A. Bouziane, A. Errachid, and F. Zaoui, Asian Pac. J. Cancer Prev. **17**, 335 (2016).
[8]F. Laidi, A. Bouziane, A. Lakhdar, S. Khabouze, M. Amrani, B. Rhrab, and F. Zaoui, Asian Pac. J. Cancer Prev. **15**, 4659 (2014).
[9]S. Mittal, H. Kaur, N. Gautam, and A. K. Mantha, Biosens. Bioelectron. **88**, 217 (2017).
[10]E. C. Porto-Mascarenhas, D. X. Assad, H. Chardin, D. Gozal, G. D. L. Canto, A. C. Acevedo, and E. N. S. Guerra, Crit. Rev. Oncol. Hematol. **110**, 62 (2017).
[11]C. F. Streckfus, D. Arreola, C. Edwards, and L. Bigler, J. Oncol. **2012**, 413256.
[12]R.-N. Zhao, Z. Feng, Y.-N. Zhao, L.-P. Jia, R.-N. Ma, W. Zhang, L. Shang, Q.-W. Xue, and H.-S. Wang, Talanta **200**, 503 (2019).
[13]A. Berezov, H.-T. Zhang, M. I. Greene, and R. Murali, J. Med. Chem. **44**, 2565 (2001).
[14]ACROBiosysteams, Human Mucin-1, Fc Tag ELISA, see https://www.acrobiosystems.com/L-380-Mucin-1.html?gclid=EAIaIQobChMIz5Wuwe6EgQMVdUd_AB1BbQZXEAAYASAAEgKlUPD_BwE.
[15]V. Agnolon, A. Contato, A. Meneghello, E. Tagliabue, G. Toffoli, M. Gion, F. Polo, and A. S. Fabricio, Sci. Rep. **10**, 3016 (2020).
[16]P. Mehrotra, J. Oral Biol. Craniofacial Res. **6**, 153 (2016).
[17]Y.-C. Syu, W.-E. Hsu, and C.-T. Lin, ECS J. Solid State Sci. Technol. **7**, Q3196 (2018).
[18]T. Wadhera, D. Kakkar, G. Wadhwa, and B. Raj, J. Electron. Mater. **48**, 7635 (2019).
[19]K.-I. Chen, B.-R. Li, and Y.-T. Chen, Nano Today **6**, 131 (2011).
[20]C.-H. Chu *et al.*, Sci. Rep. **7**, 1 (2017).
[21]Y. Cui and C. M. Lieber, Science **291**, 851 (2001).
[22]J. Kim, F. Kim, and J. Huang, Mater. Today **13**, 28 (2010).
[23]I. Sarangadharan, A. K. Pulikkathodi, C.-H. Chu, Y.-W. Chen, A. Regmi, P.-C. Chen, C.-P. Hsu, and Y.-L. Wang, ECS J. Solid State Sci. Technol. **7**, Q3032 (2018).
[24]F. Schwierz, Nat. Nanotechnol. **5**, 487 (2010).
[25]J. Sengupta and C. M. Hussain, Carbon Trends **2**, 100011 (2021).
[26]J. Xu, J. Jia, S. Lai, J. Ju, and S. Lee, Appl. Phys. Lett. **110**, 033103 (2017).
[27]P. H. Carey *et al.*, J. Electrochem. Soc. **167**, 037507 (2019).
[28]P. H. Carey, J. Yang, F. Ren, Y.-T. Liao, C.-W. Chang, J. Lin, S. J. Pearton, B. Lobo, and M. E. Leon, J. Electrochem. Soc. **166**, B708 (2019).
[29]K. Chen *et al.*, Appl. Phys. Lett. **92**, 192103 (2008).
[30]J. Yang, P. Carey IV, F. Ren, M. A. Mastro, K. Beers, S. Pearton, and I. I. Kravchenko, Appl. Phys. Lett. **113**, 032101 (2018).
[31]M. Xian *et al.*, J. Vac. Sci. Technol. B **40**, 023202 (2022).
[32]M. Xian *et al.*, J. Vac. Sci. Technol. B **39**, 033202 (2021).
[33]Z. Zhan, Certificate of Analysis: Recombinant Anti-MUC1 Antibody, Rabbit Monoclonal. SinoBiological, see https://www.sinobiological.com/antibodies/human-muc1-12123-r003.
[34]Z. Zhan, Certificate of Analysis: Recombinant Anti-Her2/ERBB2 Antibody, Rabbit Monoclonal. SinoBiological, see https://www.sinobiological.com/antibodies/human-her2-erbb2-10004-r002.
[35]C.-C. Chiang, C.-W. Chiu, F. Ren, C.-T. Tsai, Y.-T. Liao, J. F. Esquivel-Upshaw, and S. J. Pearton, J. Vac. Sci. Technol. B **41**, 012204 (2023).
[36]S.-S. Shan *et al.*, IEEE Trans. Biomed. Circuits Syst. **1**, 1362 (2020).
[37]J. Yang, P. Carey IV, F. Ren, Y.-L. Wang, M. L. Good, S. Jang, M. A. Mastro, and S. Pearton, Appl. Phys. Lett. **111**, 202104 (2017).
[38]S. Tian, K. Zeng, A. Yang, Q. Wang, and M. Yang, J. Immunol. Methods **451**, 78 (2017).
[39]M. Xian *et al.*, J. Vac. Sci. Technol. B **41**, 013201 (2023).
[40]A. M. Gown, Mod. Pathol. **21**, S8 (2008).
[41]L. F. Abrahao-Machado and C. Scapulatempo-Neto, World J. Gastroenterol. **22**, 4619 (2016).
[42]D. Baskic, P. Ristic, S. Pavlovic, and N. Arsenijevic, J. Balkan Union Oncol. **9**, 289 (2004).
[43]D. Di Gioia, M. Dresse, D. Mayr, D. Nagel, V. Heinemann, and P. Stieber, Clin. Chim. Acta **440**, 16 (2015).
[44]S. Haidar, P. B. Bhanushali, K. K. Shukla, D. Modi, C. P. Puri, S. B. Badgujar, and M. Chugh, Int. J. Biol. Macromol. **107**, 1456 (2018).
[45]P. Zhang, J. Xiao, Y. Ruan, Z. Zhang, and X. Zhang, Cancer Manag. Res. **12**, 4667 (2020).